Genetic Characterization of Cancer of Unknown Primary Using Liquid Biopsy Approaches

Noemi Laprovitera[1,2†], Irene Salamon[1,3†], Francesco Gelsomino[1,4], Elisa Porcellini[1], Mattia Riefolo[1,5], Marianna Garonzi[6], Paola Tononi[6], Sabrina Valente[1], Silvia Sabbioni[3], Francesca Fontana[6], Nicolò Manaresi[6], Antonia D'Errico[1,5], Maria A. Pantaleo[1,4], Andrea Ardizzoni[1,4] and Manuela Ferracin[1]*

[1] Department of Experimental, Diagnostic and Specialty Medicine (DIMES), University of Bologna, Bologna, Italy, [2] Department of Life Sciences and Biotechnologies, University of Ferrara, Ferrara, Italy, [3] Center for Applied Biomedical Research (CRBA), University of Bologna, Italy, [4] Divisione di Oncologia Medica, IRCCS Azienda Ospedaliero-Universitaria di Bologna, Bologna, Italy, [5] Pathology Unit, Sant'Orsola Hospital, IRCCS Azienda Ospedaliero-Universitaria di Bologna, Bologna, Italy, [6] Menarini Silicon Biosystems S.p.A, Bologna, Italy

Cancers of unknown primary (CUPs) comprise a heterogeneous group of rare metastatic tumors whose primary site cannot be identified after extensive clinical–pathological investigations. CUP patients are generally treated with empirical chemotherapy and have dismal prognosis. As recently reported, CUP genome presents potentially druggable alterations for which targeted therapies could be proposed. The paucity of tumor tissue, as well as the difficult DNA testing and the lack of dedicated panels for target gene sequencing are further relevant limitations. Here, we propose that circulating tumor cells (CTCs) and circulating tumor DNA (ctDNA) could be used to identify actionable mutations in CUP patients. Blood was longitudinally collected from two CUP patients. CTCs were isolated with CELLSEARCH® and DEPArray™ NxT and Parsortix systems, immunophenotypically characterized and used for single-cell genomic characterization with $Ampli1^{TM}$ kits. Circulating cell-free DNA (ccfDNA), purified from plasma at different time points, was tested for tumor mutations with a CUP-dedicated, 92-gene custom panel using SureSelect Target Enrichment technology. In parallel, FFPE tumor tissue was analyzed with three different assays: FoundationOne CDx assay, DEPArray LibPrep and OncoSeek Panel, and the SureSelect custom panel. These approaches identified the same mutations, when the gene was covered by the panel, with the exception of an insertion in APC gene. which was detected by OncoSeek and SureSelect panels but not FoundationOne. FGFR2 and CCNE1 gene amplifications were detected in single CTCs, tumor tissue, and ccfDNAs in one patient. A somatic variant in ARID1A gene (p.R1276*) was detected in the tumor tissue and ccfDNAs. The alterations were validated by Droplet Digital PCR in all ccfDNA samples collected during tumor evolution. CTCs from a second patient presented a pattern of recurrent amplifications in ASPM and SEPT9 genes and loss of FANCC. The 92-gene custom panel identified 16 non-synonymous somatic alterations in ccfDNA, including a deletion (I1485Rfs*19) and a somatic mutation (p.

A1487V) in *ARID1A* gene and a point mutation in *FGFR2* gene (p.G384R). Our results support the feasibility of non-invasive liquid biopsy testing in CUP cases, either using ctDNA or CTCs, to identify CUP genetic alterations with broad NGS panels covering the most frequently mutated genes.

Keywords: CTC, cell-free tumor DNA, cancer of unknown primary, liquid biopsy, precision oncology

INTRODUCTION

Malignant solid tumors that are not fully eradicated at an early stage are doomed to spread to nearby lymph nodes and organs and eventually give origin to distant metastases. A diagnosis of metastatic cancer considerably reduces the chances to eliminate the tumor and cure the patient. The metastatic process is made possible by the progressive acquirement of genetic alterations in tumor cells, which eventually become anchorage independent and self-sufficient for cell growth. Disseminated tumor cells, including circulating tumor cells (CTCs) and CTC clusters, are highly metastatic (Aceto et al., 2014), and their number in the blood correlates with patient prognosis in several cancer types (Riethdorf et al., 2007; Joosse et al., 2015; Sparano et al., 2018).

The epitome of advanced cancers could be considered a particularly aggressive metastatic disease known as cancer of unknown primary (CUP, also occult primary cancer). CUP is a rare syndrome of metastatic cancers whose primary site cannot be identified after detailed physical examinations, blood analyses, imaging, and immunohistochemical (IHC) testing (Fizazi et al., 2015). CUPs make up 3–5% of newly diagnosed cancers worldwide and represent an important clinical problem (Varadhachary and Raber, 2014; Laprovitera et al., 2021), specifically when considering that current therapeutic protocols are primary site oriented. As a final result, CUP patients receive empirical cytotoxic chemotherapy regimens and have poor prognosis [average overall survival (OS) 4–9 months, about 20% survive more than 1 year]. It has been reported that CUPs present actionable genetic alterations (Ross et al., 2015; Varghese et al., 2017), and these alterations can be identified in circulating tumor DNA (ctDNA) (Kato et al., 2017). Therefore, an improvement in CUP treatment and outcome could derive from clinical trials where patients are treated in accordance to their specific actionable mutations (Conway et al., 2019), as in NCT02628379 based on FoundationOne CDx target sequencing (Roche Foundation Medicine), or basket trials extended to CUP patients. Moreover, recent studies evidenced how CUP patients could benefit from treatment with immune checkpoint inhibitors (Haratani et al., 2019), and clinical trials have been opened and are currently recruiting (NCT04131621) or positively concluded (UMIN000030649). In this clinical trial, 56 CUP patients, of whom 45 previously treated, were treated with anti PD-1 nivolumab; the objective response rate (ORR) in the overall population was 21.4%, with a median progression-free survival (PFS) and OS of 5.1 (95% CI, 2.7–5.6) and 15.9 months (95% CI, 8.4–not reached), respectively (Tanizaki et al., 2020).

CUP genetic testing is currently limited by the scarcity of tumor biopsy material and reduced biopsy DNA quality; therefore, a liquid biopsy approach could be of the outmost interest. Several works demonstrated the utility of ctDNA and CTC testing to monitor cancer patient prognosis and guide treatment decisions (Ignatiadis and Dawson, 2014). In addition, ctDNA variant allele frequency was found to be associated with a worse prognosis in patients with metastatic disease (Pairawan et al., 2020); moreover, CTCs became an important clinical prognostic biomarker (Amintas et al., 2020) with potential application in *in vitro* (Zhao et al., 2019) and *in vivo* disease modeling (Drapkin et al., 2018) and drug testing (Yu et al., 2014). Size-based or antigen-based technologies for CTC isolation and/or enumeration have been developed in the past 10 years, each one presenting advantages and limitations (Yu et al., 2011).

CUP patients are usually diagnosed with an advanced metastatic disease; therefore, they are likely to have a high number of CTCs and CTC clusters in the circulation. Given the CUP undifferentiated status and variable presentation, it is yet to demonstrate whether CUP CTCs could be isolated using tumor antigen selection (Komine et al., 2014). In this study, we explored liquid biopsy, specifically ctDNA- and CTC-based applications, as approaches to detect CUP druggable mutations. We compared two methods to isolate CTCs, one antigen-based, size-agnostic (CELLSEARCH, Menarini Silicon Biosystems) and another antigen-agnostic, size-based (Parsortix, ANGLE plc). CTCs and ctDNA were detectable in the blood of CUP patients and analyzed for genomic alterations, which were further compared with genomic alterations identified in tumor biopsy.

MATERIALS AND METHODS

Sample Collection

Two patients (Pt#71 and Pt#95) with a diagnosis of cancer of unknown origin (CUP) were recruited at Bologna University Hospital, Italy. The study was conducted in accordance with the Declaration of Helsinki, and the protocol was approved by the Ethics Committee Center Emilia-Romagna Region— Italy (protocol 130/2016/U/Tess). Patients provided written informed consent.

Metastatic tissue from lymph node (Pt#71) and ampulla of Vater (Pt#95) was formalin-fixed and paraffin-embedded (FFPE) and used for tumor DNA collection. For Pt#71, blood sampling was performed at three different time points: (A) at diagnosis (August 2018), (B) during FOLFOX-4 treatment (stable disease, November 2018), and (C) at disease progression (May 2019). For Pt#95, blood sampling was performed at diagnosis.

Plasma separation was performed *via* centrifugation at $1,900 \times g$ for 10 min at 4°C. A variable number ($N = 2$–5) of plasma aliquots (1 ml) for each patient was collected and stored at −80°C prior to isolation of circulating cell-free DNA (ccfDNA). PBMCs were isolated from peripheral blood of Pt#95 using Ficoll-Paque Plus (17-1440-02, GE Healthcare, Chicago, IL,

United States). Briefly, after plasma depletion, an equal volume of PBS was added to the remaining blood in EDTA tubes. Following, 4 ml of diluted blood was stratified on 3 ml of Ficoll-Paque Plus and centrifuged at $400 \times g$ for 30 min at room temperature in a swinging-bucket rotor. The PBMC ring was carefully removed by pipetting and the pellet was washed with PBS and centrifuged at $100 \times g$ for 5 min. Finally, the pellet was stored at $-80°C$ prior to proceeding with DNA extraction.

CTC Isolation With CELLSEARCH and DEPArray NxT

Pt#71 and Pt#95 blood samples were collected at diagnosis. CELLSEARCH® system (Menarini Silicon Biosystems, Castel Maggiore, Italy) was used to enrich and enumerate CTCs, followed by single-cell isolation with the DEPArray® NxT system (Menarini Silicon Biosystems). Briefly, 7.5 ml of blood was loaded in CELLSEARCH Autoprep® for EpCAM-based immunomagnetic capture of CTCs, followed by immunofluorescent staining (CK-FITC, PD-L1-PE, CD45-APC, and DAPI using the CELLSEARCH CXC kit in one patient, and CK-PE, CD45-APC, and DAPI with the CELLSEARCH CTC kit in the other patient). After CTC enumeration with the CellTrack Analyzer II, the sample was loaded into a DEParray Cartridge and single CTCs and leukocytes were isolated with the DEPArray NxT system (Menarini Silicon Biosystems) from each sample. A variable number of CTCs and leukocytes, used as control, were isolated as single cells and then subjected to whole-genome amplification employing the *Ampli*1 WGA Kit (Menarini Silicon Biosystems).

CTC Isolation With the Parsortix System

For Pt#95, tumor cells were enriched from peripheral blood also using the Parsortix system (ANGLE plc, Guildford, United Kingdom). Blood cells were forced to pass through a 6.5-μm separator cassette that can capture CTCs based on their size and deformability properties. Then, to confirm the CTC nature of retained cells, we stained CTCs using a combination of anti-human EpCAM-FITC, anti-human CD45-APC (BD 561864/555485), and DAPI for cell nuclei staining. Images were acquired using a Leica DMI6000 B inverted fluorescence microscope (Leica Microsystems, Wetzlar, Germany).

DNA Extraction

DNA was extracted from the tumor area after selection by an expert pathologist, with the guidance of the hematoxylin–eosin-stained section. The DNA from different areas of FFPE unstained slides was extracted using the QIAamp DNA FFPE Tissue Kit (Cat No: 56404, Qiagen, Hilden, Germany) following the manufacturer's guidelines (as described in Cinausero et al., 2019). Normal DNA was extracted from a non-tumor area in formalin-fixed paraffin-embedded (FFPE) tissue for Pt#71 and from PBMC for Pt#95. DNA from PBMCs was extracted using the QIAamp DNA Micro kit (Cat No: 56304, Qiagen, Hilden, Germany). Ten slices of Pt#71 FFPE tumor tissue were sent to Roche Foundation Medicine (Cambridge, MA, United States)

for comprehensive genomic profile analysis with FoundationOne CDx (F1CDx) assay.

ccfDNA was purified from 1 ml of plasma by Maxwell RSC instrument (Cat No: AS4500, Promega, Madison, WI, United States) using the Maxwell RSC ccfDNA Plasma Kit (Cat No: AS1480, Promega). Genomic and ccfDNA were quantified using the Qubit 4.0 Fluorometer (Cat No: Q33238, Thermo Fisher Scientific, Waltham, MA, United States) and the Qubit dsDNA High Sensitivity Assay Kit (Cat No: Q32854, Thermo Fisher Scientific).

We assessed yields and quality of FFPE-derived gDNAs using the NGS FFPE QC Kit (Cat No: G9700B, Agilent Technologies, Santa Clara, CA, United States) according to the producer's protocol (G9700-90000, v. E1, May 2018, Agilent Technologies).

Analysis of Tumor Genetic Alterations

A 1.2-Mb custom SureSelect capture bait library (Agilent Technologies, Santa Clara, CA, United States) was designed to target 92 genes (listed in **Supplementary Table 1**), selected to be the most frequently mutated genes in CUPs, as reported in MSK Impact study CUP cohort (Zehir et al., 2017), including druggable or potentially actionable alterations. The panel was designed using Agilent SureDesign web application (v. 7.0, Agilent Technologies)[1] to cover coding exons and UTRs, with 25 flanking bases from 3' and 5' ends. This panel comprehends up to 51,466 probes included in five probe groups, with 2 × tiling density, balanced boosting, and 86% of probes with the most stringent masking. Libraries were prepared using the custom gene panel following *SureSelectXT HS/SureSelectXT Low Input Target Enrichment with Pre-Capture Pooling* protocol (G9702-90005, v. A0, June 2019, Agilent Technologies). An input of 50 ng of gDNA (normal and tumor) underwent enzymatic fragmentation according to *SureSelect Enzymatic Fragmentation* protocol (G9702-90050, Revision B0, January 2020, Agilent Technologies). Libraries from ccfDNAs of Pt #71 (A, C) and Pt#95 were prepared starting from 25 ng of DNA bypassing the fragmentation step, as described in a published application note (Barber et al., 2017). Libraries were sequenced on NextSeq 500 (Illumina) platform using High Output 2 × 75-bp flow cells. Variant calling and paired analyses (tumor vs. normal) were performed using SureCall software (v. 4.2), applying a filter for all samples at 5%, and at 1% for ccfDNAs. Somatic alterations were filtered to only keep exonic non-synonymous single-nucleotide variants (SNVs), insertions, deletions, multiple nucleotide variants, and long deletions not detected in the normal sample.

Alterations with population allele frequency (Genome Aggregation Database, GnomAD; Karczewski et al., 2020) higher than 0.5% in Non-Finnish European (NFE) population were also filtered out. All variants reported had a coverage higher than 100. Target sequencing data (92-gene custom panel) were used to assess copy number variants using panelcn.MOPS pipeline (Povysil et al., 2017). Variants triage and clinical classification was obtained with Alissa Interpret software (Agilent Technologies). Variants were also annotated using ANNOVAR (Wang et al., 2010). Bioinformatic pathogenicity prediction, reported in

---

[1] https://earray.chem.agilent.com/suredesign/

Tables 1, 2, of the identified variants was performed consulting the prediction score/outcome of SIFT (Sort Intolerated From Tolerated; Vaser et al., 2016), Polyphen2 HVAR (Polymorphism Phenotyping v2; Adzhubei et al., 2010), LRT (Likelihood Ratio Test; Chun and Fay, 2009), Mutation Taster (Schwarz et al., 2014), Mutation Assessor (Reva et al., 2011), FATHMM (Functional Analysis Through Hidden Markov Model; Shihab et al., 2013), CADD (Combined Annotation Dependent Depletion; Kircher et al., 2014), and VEST (Variant Effect Scoring Tool; Douville et al., 2016). Genes with evidence for actionability and the FDA-approved drugs reported in Tables 1, 2 were obtained consulting OncoKB (Chakravarty et al., 2017).

Single-cell genomic DNA from DEPArray NxT sorted cells, amplified using the *Ampli*1^{TM} WGA Kit, was processed to obtain Illumina-compatible libraries using the *Ampli*1^{TM} OncoSeek Panel and the *Ampli*1^{TM} LowPass kits. Conversely, tumor gDNA was directly processed with DEPArray^{TM} LibPrep and DEPArray^{TM} OncoSeek Panel kits. After sequencing on MiSeq platforms, raw data were analyzed using assay-specific applications on the MSBiosuite platform (Menarini Silicon Biosystems).

FFPE tumor tissue of Pt#71 was eligible for genetic testing using FoundationOne CDx (F1CDx) assay. F1CDx is performed exclusively as a laboratory service using DNA extracted from FFPE tumor samples. A library was prepared with a hybrid capture−based target enrichment approach and whole−genome shotgun library construction to detect substitutions, indels, copy number alterations, and selected rearrangements in a total of 324 genes. Sequencing was performed using the Illumina HiSeq 4000 platform, obtaining a $>500 \times$ median coverage. F1CDx specimens were also simultaneously profiled for tumor mutation burden (TMB) and microsatellite instability (MSI) status (further technical information is available at https://www.foundationmedicine.com/genomic-testing/foundation-one-cdx).

Droplet Digital PCR Validation

Droplet Digital PCR technology (Bio-Rad, Hercules, CA, United States) along with Mutational and Copy Number Determination assays (Bio-Rad) were used to validate specific alterations in both genomic and ccfDNAs. A Copy Number Variation assay was used to assess the amplification of *FGFR2* gene (dHsaCB2500320, Bio-Rad) using *RPP30* as reference gene (dHsaCP2500350, Bio-Rad). A digestion with *Hae*III restriction enzyme was performed during ddPCR, according to the manufacturer's instruction. Mutational assay for wild-type and mutated *ARID1A* (p.R1276*) was performed with a custom IDT assay (02516372). For this assay, DNA digestion with *Hin*dIII restriction enzyme was performed only for gDNA. Probe-based Droplet Digital PCR experiment was performed according to the manufacturer's instruction and thermal cycling conditions were 95°C for 10 min, 94°C for 30 s and 58°C for 1 min for 40 cycles, 98°C for 10 min, and an infinite hold at 4°C (ramping rate reduced to 2%). Droplet selection was performed individually for each well using QuantaSoft software v 1.7 (Bio-Rad) obtaining the final copy number variation or the wild-type/mutated allele fractions.

RESULTS

Case Presentation

Pt#71

A 49-year-old woman with a history of primary biliary cholangitis (PBC) was admitted at Bologna University Hospital in June 2018 due to enlarged left cervical lymph nodes associated with severe asthenia, pruritus, and fever. A contrast-enhanced computed tomography (CT) scan showed multiple pathologic abdominal (epigastrium, mesogastrium, stomach curvature, hepatic hilum, pancreatic, and retroperitoneal regions) and left supraclavicular lymph nodes, confirmed also by a F-Fluorodeoxyglucose positron emission tomography/computed tomography (18-F-FDG PET/CT) scan. The patient underwent abdominal surgery leading to the excision of two lymph nodes. Pathological examination confirmed the presence of nodal metastasis from adenocarcinoma.

Immunohistochemistry staining reported positivity for keratin 7, keratin 20, and CDX2, and negativity for neuroendocrine markers (chromogranin, synaptophysin, and CD56). Therefore, the conclusive pathological diagnosis was suggestive of lymph node metastasis from adenocarcinoma of the gastrointestinal tract. Esophagogastroduodenoscopy (EGDS) and pancoloscopy (PC) failed to identify any neoplastic lesion. In addition, molecular analyses for the determination of MSI, HER2, ALK, and PD-L1 status (by IHC); *KRAS*, *NRAS*, *BRAF* mutational status and *MGMT* methylation status (by pyrosequencing); and *ROS1* and *MET* (by FISH) were all negative. Among the serum oncomarkers, the positive ones were Ca19.9 (291 U/ml, n.v < 40 U/ml), Ca125 (130.9 U/ml, n.v < 35 U/ml), and NSE (34 µg/L, n.v < 12 µg/L).

Taking into account the history of PBC and its association with a higher risk of cholangiocarcinoma, a magnetic resonance cholangiopancreatography (MRCP) and MRI with contrast was performed and ruled out the presence of any tumor lesion. Then, the patient was treated with FOLFOX-4 as first-line treatment every 2 weeks up to 11 courses, obtaining a partial response. A maintenance treatment based on De Gramont regimen (FULCV) was continued for four courses followed by a worsening of patient's clinical condition and the appearance of pleural and abdominal effusions. Blood was collected for CTC analysis with CELLSEARCH and DEPArray at November 2018. Treatment with Pazopanib, a novel multi-kinase inhibitor (VEGFR1, VEGFR2, VEGFR3, PDGFR, FGFR, c-Kit, and c-Fms/CSF1R), was proposed due to the presence of *FGFR2* amplification (F1CDx testing). However, death occurred in June 2019 due to progressive disease and hepato-renal syndrome.

Pt#95

A 63-year-old woman was admitted at Bologna University Hospital in February 2019 due to an edema of the upper limb. Echo-Doppler scanning revealed thrombosis in basilica, axillary, subclavian, internal jugular, and external jugular veins. The patient experienced weight loss, asthenia, nausea, and cough.

A contrast-enhanced total body CT showed the presence of supra- and infradiaphragmatic enlarged lymph nodes associated

TABLE 1 | Mutation report of tumor, ccfDNA, and CTCs from Pt#71.

Gene	Position	Coding change	Amino acidic change	SureSelect 92-gene panel (Agilent Technologies) Tumor FFPE	SureSelect 92-gene panel (Agilent Technologies) ccfDNA at diagnosis	SureSelect 92-gene panel (Agilent Technologies) ccfDNA at PD	Foundati-One CDx (Roche) Tumor FFPE	Ampli1™ OncoSeek and LowPass Kit (Menarini Silicon Biosystem) CTCs	DEPArray™ OncoSeek and LowPass Kit (Menarini Silicon Biosystem) Tumor FFPE	Pathogenicity Prediction SIFT (Vaser et al., 2016)	Polyphen2 (Adzhubei et al., 2010)	LRT (Chun and Fay, 2009)	Mutation Taster (Schwarz et al., 2014)	Mutation Assessor (Reva et al., 2011)	FATHMM (Shihab et al., 2013)	CADD (Kircher et al., 2014)	VEST3 (Douville et al., 2016)	Actional genes/approved drugs [OncoKB (Chakravarty et al., 2017)]
APC	chr5:112840254	4607insA	p.T1556fs*3	9.8%	22.6%	29.9%	ND	90.2%-99.2%	14.0%	–	–	–	–	–	–	–	–	–
ARID1A	chr1:26773456	c.C3826T	p.R1276X	8.9%	28.5%	22.8%	7.3%	NI	NI	–	–	–	DC	–	–	HF	–	–
ERBB3	chr12:56085144	c.C384A	p.S128R	9.8%	20.7%	20.4%	8.5%	NI	NI	–	PS	DT	DC	NFL	TL	BG	HF	–
NTRK1	chr1:156881475	C2206T	p.Q736X	8.3%	26.0%	22.3%	7.6%	NI	NI	DT	–	DT	DC	–	–	HF	–	–
KEAP1	chr19:10499630	c.G404A	p.R135H	9.0%	22.6%	19.5%	7.0%	NI	NI	TL	PD	DT	DC	NFL	TL	HF	HF	–
PALB2	chr16:23629735	C2419T	p.P807S	9.0%	19.1%	16.6%	6.0%	NI	NI	TL	BG	NL	PM	NFN	TL	BG	BG	Level 1/Olaparib*
KMT2C	chr7:152265209	c.C1013T	p.S338L	ND	5.5%	4.3%	NI	NI	NI	TL	PD	U	DC	NFL	DG	BG	BG	–
KMT2C	chr7:152247975	c.C2459T	p.T820I	ND	1.1%	1.1%	NI	NI	NI	DT	PS	DT	DC	NFL	DG	HF	–	–
PTPRD	chr9:8404618	c.T2908G	p.L970V	ND	5.1%	3.5%	NI	NI	NI	–	PD	DT	DC	FCM	TL	BG	HF	–
TP53	chr9:8404618	c.T316C	p.C106R	ND	2.1%	ND	ND	ND	ND	DT	PD	DT	DC	FCM	DG	HF	HF	Levels 1–3/no drug
TP53	chr17:7674251	c.G315C	p.M105I	ND	1.8%	ND	ND	ND	ND	DT	PD	DT	DC	FCM	DG	HF	HF	Levels 1–3/no drug
TP53	chr17:7674252	c.A355G	p.I119V	ND	1.7%	ND	ND	ND	ND	DT	PD	DT	DC	FCM	DG	HF	HF	Levels 1–3/no drug
TP53	chr17:7674212	c.C9G	p.C3W	ND	1.2%	ND	ND	ND	ND	DT	PD	DT	DC	FCM	DG	BG	HF	Levels 1–3/no drug
ALK	chr2:29328463	c.A1301G	p.K434R	ND	ND	7.0%	ND	OTR	OTR	–	BG	U	DC	NFN	TL	HF	BG	Level 1/Lorlatinib, Brigatinib*
EPHA5	chr4:65420551	c.A1417C	p.T473P	ND	ND	8.3%	NI	NI	NI	TL	PS	NL	DC	NFL	TL	BG	HF	–
FAT1	chr4:186707744	c.A2084C	p.N695T	ND	ND	2.6%	NI	NI	NI	TL	BG	NL	PM	NFN	TL	BG	BG	–
MGA	chr15:41736268	c.T4004C	p.L1335P	ND	ND	1.6%	NI	NI	NI	DT	PD	NL	DC	NFN	TL	BG	HF	–
KMT2C	chr7:152248206	c.C2228T	p.P743L	ND	ND	1.6%	NI	NI	NI	TL	BG	NL	PM	NFN	DG	BG	BG	–
KMT2C	chr7:152235897	c.C2689T	p.R897X	ND	ND	1.4%	NI	NI	NI	–	–	–	DC	–	–	HF	–	–
PTPRD	chr9:8389280	c.A3117C	p.Q1039H	ND	ND	6.8%	ND	NI	NI	–	PD	DT	DC	FCM	DG	BG	HF	–
ABL1	chr9:133760790	c.C3113T	p. A1038V	NI	NI	NI	52.8%	OTR	OTR	–	BG	–	–	NFN	–	HF	–	–
GRM3	chr7:86415916	c.C808T	p.R270C	NI	NI	NI	7.0%	NI	NI	–	PS	–	–	FCM	–	HF	–	–
MAP3K1	chr5:56177843	c.C2816G	p.S939C	NI	NI	NI	49.6%	NI	NI	–	BG	–	–	–	–	HF	–	–
MSH3	chr5:80149992	c.A2857T	p.M953L	NI	NI	NI	46.1%	NI	NI	–	PD	–	–	FCM	–	HF	–	–
MSH6	chr2:48028273	c.G3151A	p.V1051I	NI	NI	NI	50.0%	OTR	OTR	–	BG	–	–	NFL	–	BG	–	–
PTPRO	chr12:15475691	c.G31T	p.A11S	NI	NI	NI	52.2%	NI	NI	–	BG	–	–	NFN	–	BG	–	–

*NI, not included; ND, not detected; OTR, out of target region; TL, tolerated; DT, deleterious; BG, benign; PD, Probably Damaging; PS, Possibly damaging; U, Unknown, NL, normal; DC, Disease causing; PM, polymorphism; NFN, non-functional neutral; NFL, non-functional low; FCM, functional medium; DG, Damaging; HF, harmful. *Approved for cancer types different from CUP.*

TABLE 2 | Mutation report of tumor, ccfDNA and CTCs from Pt#95.

Gene	Position	Coding change	Amino acidic change	SureSelect 92-gene panel (Agilent Technologies) ccfDNA at diagnosis	SureSelect 92-gene panel (Agilent Technologies) Tumor FFPE	Ampli1 OncoSeek and LowPass Kit (Menarini Silicon Biosystem) CTCs	Pathogenicity Prediction SIFT (Vaser et al., 2016)	Polyphen2 (Adzhubei et al., 2010)	LRT (Chun and Fay, 2009)	Mutation Taster (Schwarz et al., 2014)	Mutation Assessor (Reva et al., 2011)	FATHMM (Shihab et al., 2013)	CADD (Kircher et al., 2014)	VEST3 (Douville et al., 2016)	Actional genes/drugs [OncoKB (Chakravarty et al., 2017)]
ARID1A	chr1:26774679	c.4454_4457delTACA	p.I1485Rfs*19	32.6%	25%	NI	-	-	-	-	-	-	-	-	-
ARID1A	chr1:26774687	c.C4460T	p.A1487V	33.2%	27%	NI	TL	BG	DT	DC	NFN	TL	BG	HF	-
SPEN	chr1:15937527	c.G10391C	p.G3464A	31.0%	24%	NI	TL	BG	-	DC	NFL	TL	BG	BG	-
PIK3CG	chr7:106872869	c.G2218A	p.E740K	22.0%	8%	NI	TL	BG	NL	DC	NFL	TL	BG	BG	-
FGFR2	chr10:121515254	c.G814A	p.G272R	19.0%	NC	OTR	DT	PD	DT	DC	FCM	DG	HF	HF	Level 4/Debio1347, AZD4547, BGJ398, Erdafitinib
KMT2D	chr12:49031574	c.G13131A	p.W4377X	17.0%	FLQ	NI	DT	–	NL	DC†	–	–	HF	–	Level 3/no drug
FAT1	chr4:186621042	c.A5544C	p.Q1848H	13.1%	NC	NI	TL	PD	DT	DC	NFL	TL	BG	HF	–
KMT2C	chr7:152265180	c.G1042A	p.D348N	9.8%	FLQ	NI	TL	PD	U	DC	NFL	DG	BG	BG	–
KMT2C	chr7:152248140	c.A2294G	p.E765G	7.8%	ND	NI	TL	BG	DT	DC	NFL	DG	BG	BG	–
KMT2C	chr7:152235876	c.C2710T	p.R904X	7.5%	FLQ	NI	TL	–	NL	DC	–	–	HF	–	–
KMT2C	chr7:152235929	c.G2657A	p.R886H	6.8%	ND	NI	DT	PS	DT	DC	FCM	DG	HF	BG	–
KMT2C	chr7:152235861	c.A2725G	p.R909G	6.6%	ND	NI	TL	PD	DT	DC	FCM	DG	BG	HF	–
KMT2C	chr7:152248143	c.C2291T	p.S764F	4.9%	FLQ	NI	DT	BG	NL	DC	NFL	DG	BG	BG	–
KMT2C	chr7:152265209	c.C1013T	p.S338L	4.9%	ND	NI	TL	PD	U	DC	NFL	DG	BG	BG	–
KMT2C	chr7:152273774	c.G943A	p.G315S	4.9%	NC	NI	DT	PD	DT	DC	FCM	TL	HF	HF	–
KMT2C	chr7:152247966	c.T2468C	p.I823T	2.3%	NC	NI	TL	PD	DT	DC	NFL	DG	BG	HF	–
MGA	chr15:41767261	c.C8552T	p.P2851L	NC	5.20%	NI	TL	PS	NL	DC	NFN	DG	BG	BG	–
KMT2C	chr7:152163206	c.C10371A	p.D3457E	NC	6.30%	NI	TL	BG	NL	DC	NFL	DG	BG	BG	–
PTPRD	chr9:8521304	c.G904A	p.E302K	NC	5.00%	NI	–	PD	DT	DC	FCM	TL	HF	HF	–
ASXL2	chr2:25743628	c.G1929T	p.Q643H	NC	5.10%	NI	DT	PD	NL	DC	FCM	TL	BG	BG	–

NI, not included; NC, not covered region; FLQ, filtered for low quality; ND, not detected; OTR, out of target region; TL, tolerated; DT, deleterious; BG, benign; PD, Probably Damaging; PS, Possibly damaging; U, Unknown, NL, normal; DC, Disease causing; NFN, non-functional neutral; NFL, non-functional low; FCM, functional medium; DG, Damaging; HF, harmful. †Known to be disease causing.

with edema and diffuse suffusion of mesenteric and perivisceral tissues suggestive of peritoneal carcinosis, confirmed also by a 18F-FDG-PET/CT scan.

A CT-guided biopsy of a left paraortic lymph node led to a pathological diagnosis of node metastasis from poorly differentiated carcinoma with microglandular and signet-ring architecture. At immunohistochemistry, cells presented a focal positivity for K7 and CDX2 and negativity to K20 and synaptophysin. The immunophenotypical findings suggested to suspect a gastric primary tumor. Blood was collected for CTC analysis with CELLSEARCH and DEPArray and Parsortix at December 2019.

In May 2019, molecular analyses for the determination of MSI and HER2 status (by IHC) were negative, as well as KRAS, NRAS, BRAF, mutational status, and MGMT methylation status (by pyrosequencing). The patient underwent EGDS with ecoendoscopy, which found a suspicious area in the ampulla of Vater. Histological examination confirmed the presence of poorly differentiated adenocarcinoma with mixed, micro-glandular pattern, and signet-ring cells and a lymphangitic infiltration of the mucosa of duodenal type. IHC analysis reported a strong immunoreactivity to MUC1, MUC5AC, MUC6, and a complete negativity to MUC2 in addition to the previously identified K7$^+$/K20$^-$/CDX2$^+$ profile, suggesting a likely bilio-pancreatic origin.

Starting from May 2019, the patient was treated with FOLFOX-4 regimen up to nine cycles, obtaining an initial partial response. In October 2019, the patient was admitted at the Emergency room of the Bologna University Hospital due to dyspnea and bilateral pleural effusion. The patient underwent pleural drainage and cytological examination, followed by video-assisted thoracoscopy and pleurodesis. The cell block was tested by IHC and the identified tumor cells were found to be reactive for BEREP4, K7, and CDX2 and negative for TTF1 and calretinin. Molecular analysis on pleural-derived cytological specimen was performed in the diagnostic setting. The analysis reported a pathogenic alteration in FGFR2 gene (c.1150G > A, p. Gly384Arg, AF:33.4%); no gene amplification or fusion was detected. In December 2019, the patient started weekly gemcitabine regimen as second-line treatment. After 2 weeks from the first administration, the patient had uncontrolled ascitic effusion. Abdominal CT with and without contrast showed progressive disease due to evident radiological signs of peritoneal carcinosis. The patient died in January 2020 due to further progressive disease.

Identification and Characterization of CTCs From CUP Patients Using CELLSEARCH and DEPArray or Parsortix Systems

CTCs from patients' peripheral blood were isolated by combining CELLSEARCH and the DEPArray system. For Pt#71, 66 (CK$^+$/CD45$^-$/DAPI$^+$) cells (none of which was positive for PD-L1) were captured with immunomagnetic beads. The isolated cells were then loaded on DEPArray that retrieved n = 12 CTCs.

Three CTCs and one leukocyte as control were subjected to single-cell whole-genome amplification and sequencing.

For Pt#95, CELLSEARCH captured 133 CTCs cells (defined as above) from which DEPArray recovered 34 putative CTCs (**Figure 1** and **Supplementary Figure 1**). A total number of 32 CTCs and four leukocytes ware subjected to single-cell whole-genome amplification, and 10 CTCs passed quality control criteria for low-pass whole-genome analysis.

Pt#95 whole blood was also used to isolate CTCs with the Parsortix system (ANGLE plc). Large cells were isolated with a 6.5 μm Parsortix cassette. Some EpCAM-positive and CD45-negative CTCs were captured in the cassette (**Figure 2**), together with EpCAM-positive and CD45-positive cells of unknown significance (**Figure 2**).
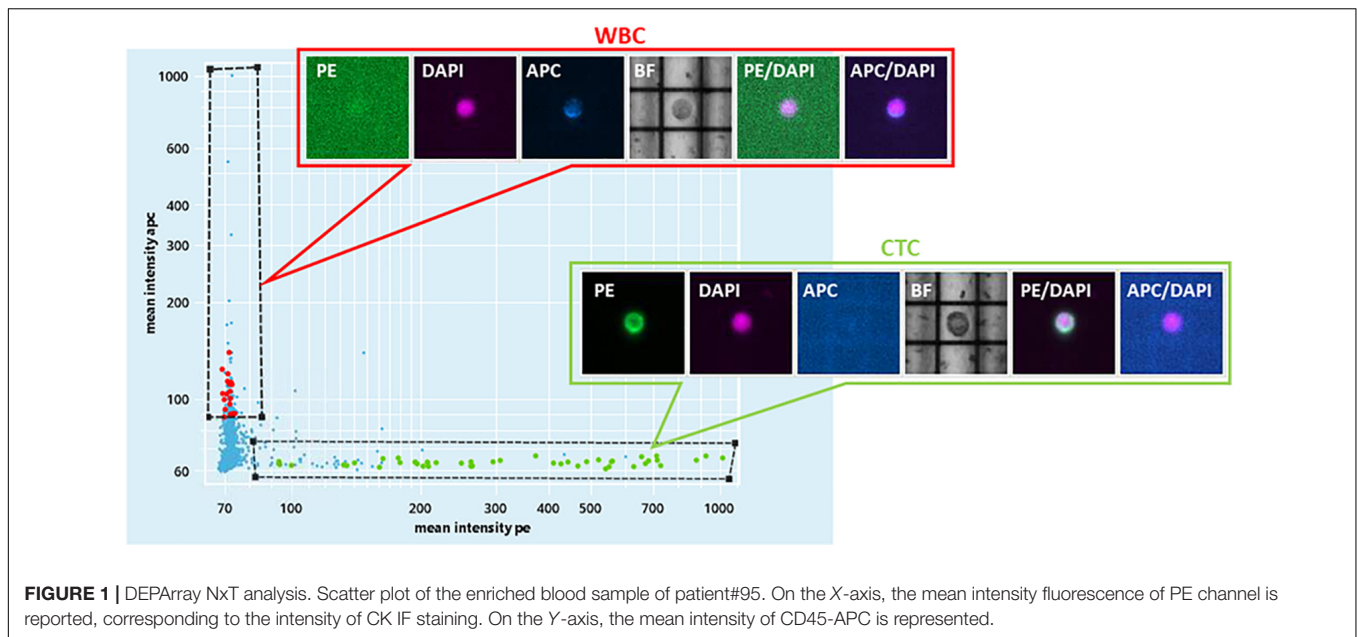
Mutational Analysis of CTCs, ctDNA, and Tumor
Pt#71

F1CDx testing reported the amplification of FGFR2 (Copy Number, CN: 49) and CCNE1 (CN: 8) genes along with a somatic variant in ARID1A gene (p.R1276*) with an allele frequency (AF) of 7.3%. Moreover, F1CDx reported an intermediate tumor mutational burden (13 mutations/Mb). Single-cell genome-wide characterization of CTCs (Ampli1 LowPass, Menarini Silicon Biosystems) allowed sub-chromosomal losses detection, including a LOH region comprising the APC gene, and pattern of extensive gains, including FGFR2 and CCNE1 genes (**Figure 3**).

The same alterations were confirmed on bulk tumor DNA. Moreover, targeted sequencing (Ampli1 OncoSeek panel, Menarini Silicon Biosystems) was able to detect the presence of FGFR2 amplification in 3/3 CTCs and the inactivating homozygous somatic variant in APC gene (p.T1556Nfs*3, AF: 90.2–99.2%). The APC somatic variant, which was missed by F1CDx, was detected (**Figure 3**) in two out of three analyzed CTCs, while the third CTC shows no coverage in the APC region (L5589, grayed out), in agreement with the deletion detected by the LowPass copy number profile in this cell, and a single-WBC control from the same sample (L5601) was wild type, as expected. The tumor gDNA target sequencing (DEPArray OncoSeek panel, Menarini Silicon Biosystems) confirmed the FGFR2 amplification and reported the same frameshift variant in APC, even though with a lower allele frequency (p.T1556Nfs*3, AF: 14%), likely due to contamination by normal cells. The single-copy homozygous variant in APC found in CTCs is coherent with a ~15% variant frequency in the presence of 70% of normal cells in FFPE. Indeed, when setting the contamination parameter to 70% in the FFPE low-pass analysis, the bioinformatic pipeline was able to call, out of the increased noise, some CNA regions similar to those detected in CTCs, which were otherwise undetectable without the correction factor (**Supplementary Figure 2**).

The SureSelect 92-gene custom panel detected the APC insertion in bulk tumor DNA (AF:9.8%) and also in circulating cfDNAs analyzed at two different time points (ccfDNA at diagnosis, AF: 22.6% and ccfDNA at the progression of the disease, AF:29.9%). The tool panelcn.MOPS (Povysil et al., 2017) used to analyze target sequencing data confirmed the

FIGURE 1 | DEPArray NxT analysis. Scatter plot of the enriched blood sample of patient#95. On the *X*-axis, the mean intensity fluorescence of PE channel is reported, corresponding to the intensity of CK IF staining. On the *Y*-axis, the mean intensity of CD45-APC is represented.

FGFR2 and *CCNE1* gene amplification reporting a copy number alteration higher than four in both genes; however, no *APC* loss was detected. Moreover, we confirmed the mutation in *ARID1A* gene (p.R1276*), *ERBB3* (p.S128R), *KEAP1* (p.R135H), *PALB2* (p.P807S), and *NTRK1* (p.Q736X), previously reported by F1CDx, both in the tumor and in the ccfDNAs. All detected variants and CNVs are listed in **Tables 1**, **3**.

In **Table 1**, we reported other mutations detected by F1CDx in genes not included in the custom panel and some variants detected in ccfDNAs not observed in the tumor. Of note, we observed mutations in *ALK* (p.K434R, AF:7%), *EPHA5* (p.T473P, AF: 8.3%), *PTPRD* (p.Q1039H, AF:6.8%), and other alterations at lower frequency.

Droplet Digital PCR technology validated the *ARID1A* mutation (**Figure 4A** and **Supplementary Figure 3A**) and the *FGFR2* amplification (**Figure 4B** and **Supplementary Figure 3B**) in bulk tumor DNA and in longitudinally collected ccfDNAs at three different time points of disease evolution. Of note, the frequency of *ARID1A* mutation decreases at time point B, during FOLFOX-4 treatment, then it increases during the progression of the disease, while the *FGFR2* amplification has a decreasing trend in terms of copy number value during disease progression. The Variant Allele Frequency reported by target sequencing at two time points was found to be consistent with the Fractional Abundance (FA% = mutated copies/mutated copies + wild-type copies) measured by ddPCR.

Pt#95

Single-cell whole-genome characterization of 10 CTCs detected a recurrent amplification signal in the regions of *ASPM* and *SEPT9* genes and a deletion including *FANCC* gene in all analyzed CTCs (**Supplementary Figure 4**), as shown in the CNV profile clustering in **Figure 5**. CTCs and bulk tumor DNA-targeted sequencing (*Ampli*1 OncoSeek Panel, Menarini

Silicon Biosystems) reported no somatic mutation in the regions covered by the panel.

Target sequencing performed on ccfDNA and tumor FFPE tissue with the 92-gene custom panel identified 16 non-synonymous, somatic genetic alterations not detected in the normal cells in the ccfDNA and 8 in the tumor DNA (**Table 2**), including *ARID1A* deletion (I1485Rfs*19, AF: 32.6%) and mutation (p. A1487V, AF: 33.2%) and a mutation in *FGFR2* gene (p.G272R, AF:19%). Of note, mutational analysis performed in the diagnostic setting (obtained with Oncomine Comprehensive Assay by Thermo Fisher Scientific) reported the same mutation in *FGFR2* gene; no amplifications or deletions were detected with Agilent custom panel, but regions including *ASPM*, *SEPT9*, and *FANCC* genes were not captured.
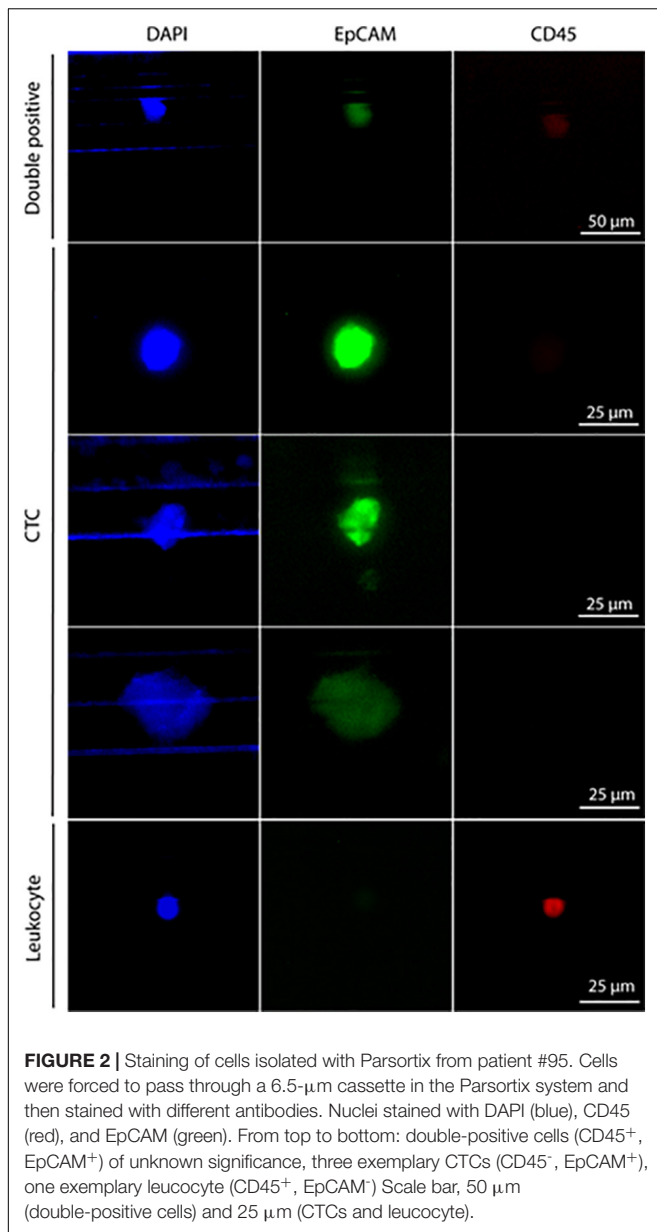
DISCUSSION

The identification of driver and actionable genetic alterations is crucial to broaden the treatment choices of cancer patients. This is particularly relevant for patients with CUP, who have reduced access to targeted and immunotherapies. One main reason resides in treatment protocols being designed in a tumor-gnostic way. Furthermore, CUPs are characterized by scarce availability of tumor material for genetic testing, due to the extensive use of tissue slices in immune-phenotypic testing required for diagnostic procedures.

In this pilot study, we took advantage of liquid biopsy approaches to genetically characterize CUP tumors using both CTCs and DNA as a source of tumor DNA, with the aim to identify druggable genetic alterations.

The isolation and counting of CTCs is becoming an important tool to evaluate aggressiveness and prognosis of different solid tumors. The CELLSEARCH system (Menarini Silicon
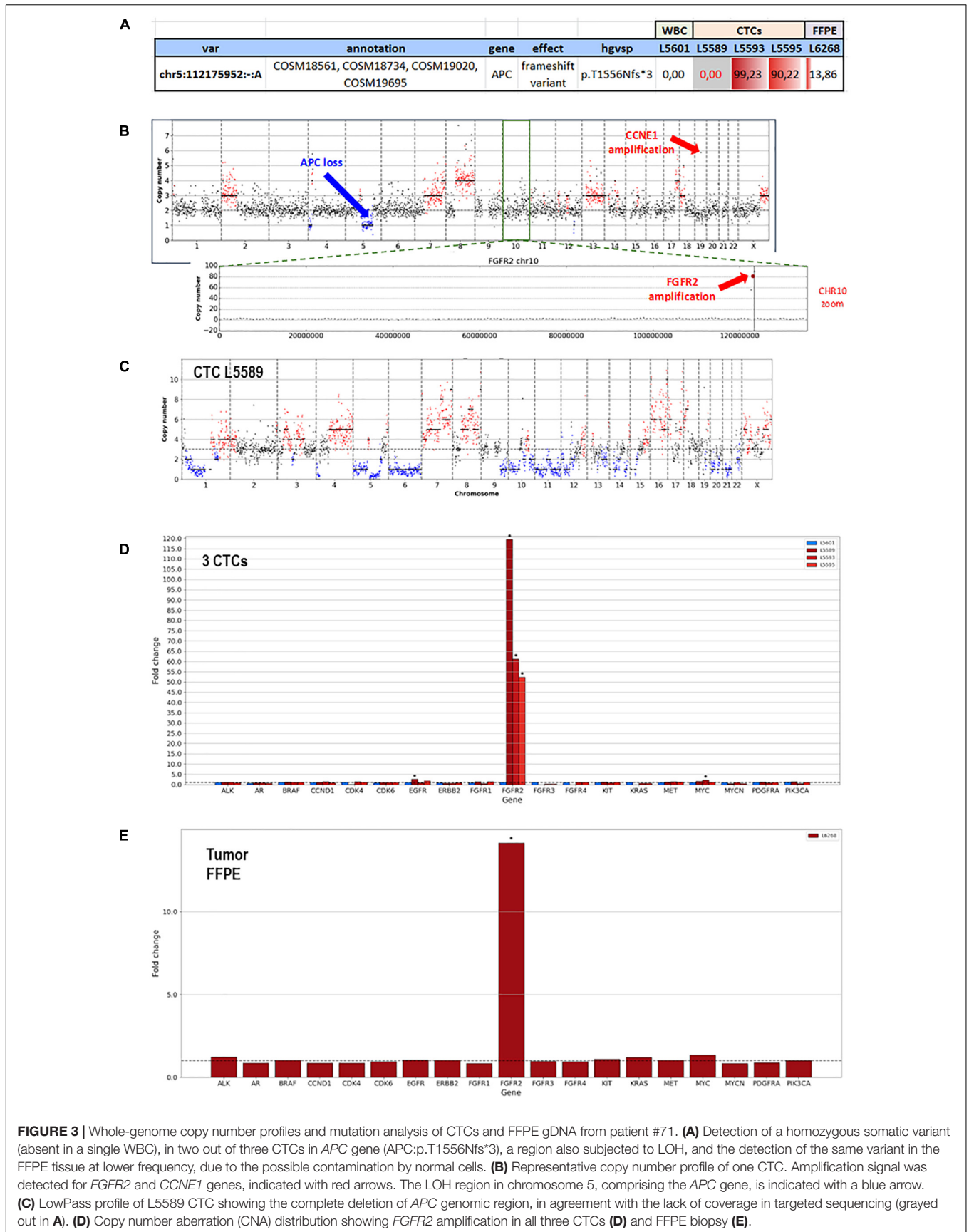
FIGURE 2 | Staining of cells isolated with Parsortix from patient #95. Cells were forced to pass through a 6.5-μm cassette in the Parsortix system and then stained with different antibodies. Nuclei stained with DAPI (blue), CD45 (red), and EpCAM (green). From top to bottom: double-positive cells (CD45+, EpCAM+) of unknown significance, three exemplary CTCs (CD45-, EpCAM+), one exemplary leucocyte (CD45+, EpCAM-) Scale bar, 50 μm (double-positive cells) and 25 μm (CTCs and leucocyte).

Recently, CTC isolation methods based on label-free systems were also developed. In one patient, we used the Parsortix system (ANGLE plc) for the size-based enrichment of CTCs from peripheral blood of CUP patients. This approach ensured a size-based selection of CTCs without the need of specific markers, which is a potential issue when isolating these cells from CUP patients. Some CTCs enriched with the Parsortix system proved to be positive for EpCAM marker, therefore confirming their epithelial origin, although no genetic confirmation could be produced. We also detected cells that co-express hemato-epithelial markers, as previously reported for a subpopulation of epithelial ovarian cancer tumor cells (Akhter et al., 2018). In this paper, the authors proposed a cell–cell fusion theory to explain the origin of these peculiar cell population. Indeed, EpCAM+ and CD45+ cells show more invasive mesenchymal properties and overexpress genes related to drug resistance, anti-apoptosis, and stemness. The detection of cells with these characteristics in circulation could be associated with CUP highly invasive phenotype and deserves further investigations.

CTCs and ccfDNA were used for CUP genetic testing. Our results from two longitudinally monitored patients suggested that CTCs and ctDNA can be isolated from the blood of CUP patients and are suitable for genetic characterization. FFPE tumor tissue was used to validate the liquid biopsy results. In addition, we analyzed and compared different targeted sequencing approaches applied to tumor FFPE tissue, CTCs, and ccfDNA: FoundationOne CDx (Roche Foundation Medicine), OncoSeek Panels (*Ampli*1 and DEPArray OncoSeek Panels, Menarini Silicon Biosystems), and an in-house developed, Agilent SureSelect panel, focusing on 92 genes frequently mutated in CUPs and metastatic solid tumors. The comprehensive genomic analysis was highly overlapping among the different approaches, when the region was covered by all panels. Clearly, these three different technologies cover a different number of genes and hot spot regions, which explains the differential detection of some variants.

Interestingly, both CUP patients presented actionable *FGFR2* aberrations. Specifically, a ~80-fold copy number amplification (Pt#71) and a gene mutation (Pt#95), both at the tumor and CTC/ctDNA level, suggest a potential implication of this pathway in tumor progression and aggressiveness (Dienstmann et al., 2014). FGFR2 is a member of the fibroblast growth factor receptor family, whose signaling pathway activates downstream effectors that play a crucial role in cell proliferation, survival, and migration (Turner and Grose, 2010). *FGFR2* rearrangements have been detected in 10–15% of intrahepatic cholangiocarcinomas (Arai et al., 2014; Silverman et al., 2019), amplifications in up to 15% of gastric cancers (Deng et al., 2012; Seo et al., 2017) and point mutations in about 10% of endometrial cancers (Byron et al., 2012); moreover, *FGFR2* amplification has also a prognostic significance in gastric cancers (Chang et al., 2014; Seo et al., 2017). Of note, in longitudinal ccfDNAs from Pt#71, we observed a progressive reduction of *FGFR2* CN during treatments, which mirrors the initial partial response. Taking into account the chemo-naïve status of the two patients and the unavailability of clinical trials testing multi-kinase or FGFR2 inhibitors in CUP patients, the patients were treated

Biosystems) is to date the only platform cleared by the FDA for detecting and enumerating CTCs in metastatic breast, prostate, and colorectal cancer patients, while other technologies are at preclinical and clinical stages of development. CTC count as measured by CELLSEARCH System proved to have prognostic value in different metastatic solid tumors, including breast (Cristofanilli et al., 2004), colorectal (Cohen et al., 2008), and gastric cancers (Matsusaka et al., 2010). In addition, the detection of one or more CTCs using this system was found to predict early recurrence and a worse prognosis in chemo naïve patients with non-metastatic breast cancer (Lucci et al., 2012). A considerable number of CTCs were detected in the two CUP patients enrolled in our study, and they were successfully enriched and enumerated by CELLSEARCH and isolated with DEPArray for downstream molecular analysis (*Ampli*1 kit).

FIGURE 3 | Whole-genome copy number profiles and mutation analysis of CTCs and FFPE gDNA from patient #71. **(A)** Detection of a homozygous somatic variant (absent in a single WBC), in two out of three CTCs in *APC* gene (APC:p.T1556Nfs*3), a region also subjected to LOH, and the detection of the same variant in the FFPE tissue at lower frequency, due to the possible contamination by normal cells. **(B)** Representative copy number profile of one CTC. Amplification signal was detected for *FGFR2* and *CCNE1* genes, indicated with red arrows. The LOH region in chromosome 5, comprising the *APC* gene, is indicated with a blue arrow. **(C)** LowPass profile of L5589 CTC showing the complete deletion of *APC* genomic region, in agreement with the lack of coverage in targeted sequencing (grayed out in **A**). **(D)** Copy number aberration (CNA) distribution showing *FGFR2* amplification in all three CTCs **(D)** and FFPE biopsy **(E)**.

TABLE 3 | Copy number (CN) alterations detected in Pt#71.

		SureSelect 92-gene panel (Agilent Technologies)	SureSelect 92-gene panel (Agilent Technologies)	FoundatiOne CDx™ (Roche)	Ampli1 OncoSeek and LowPass Kit (Menarini Silicon Biosystem)	DEPArray™ OncoSeek and LowPass Kit (Menarini Silicon Biosystem)
Gene	Alteration	Tumor FFPE (CN)	ccfDNAs (CN)	Tumor FFPE (CN)	CTC (CN)	Tumor FFPE (CN)
FGFR2	Amplification	>4	>4	49	> 80	82
CCNE1	Amplification	>4	>4	8	6	5
APC	Loss/deletion	Not detected	Not detected	Not detected	Detected	Detected

with platinum salts and fluoropyrimidines, as suggested by the current guidelines.

Pt#71 also presented an amplification in *CCNE1* (Cyclin E1) gene, which is known to be associated with poor prognosis in ovarian and triple-negative breast cancer, probably involved in the emergence of resistance to chemotherapy (Nakayama et al., 2010; Huang et al., 2020).

Another common genetic feature of the two tested CUP tumors was the presence of alterations in *ARID1A* gene, which is a tumor suppressor gene encoding the DNA-binding subunit

FIGURE 4 | Kinetics of mutated fractional abundance and CNV in longitudinal ccfDNAs measured by Droplet Digital PCR. The graph in **(A)** illustrates *ARID1A* mutated fractional abundance (p.R1276X) during patient's follow-up. This value decreases during treatment and later rises at the worsening of patient's conditions; on the contrary, when monitoring *FGFR2* amplification at the same time points, as reported in **(B)**, a decreasing trend was detected from the diagnosis to disease progression.

of the chromatin remodeler complex SWI/SNF (Trizzino et al., 2018). Despite not being druggable, this gene is the most frequently mutated chromatin regulator across all human cancers (Kadoch et al., 2013) and its loss impairs RNA polymerase II (RNAPII) pausing. Compromised RNAPII pausing results in transcriptional dysregulation of active genes, such as *TP53* and *ESR1*, which could explain the oncogenic effects of ARID1A loss (Trizzino et al., 2018). The recurrence of these mutation in both reported cases open an interesting prospective on the role of ARID1A in regulating the aggressiveness of CUPs. Of note, when longitudinally evaluated in ccfDNAs of Pt#71, the Fractional Abundance of *ARID1A* mutation (p.R1276*) decreased during treatment and then increases at disease progression, suggesting its potential involvement in disease worsening. Moreover, we noticed that in ccfDNAs at diagnosis and disease progression, in which the Fractional Abundance of $ARID1A_{mut}$ was high, there was also the emergence of novel mutations in *TP53, ALK, EPHA5, FAT1*, and *MGA* genes, not detected in the tumor biopsy. *In vitro* experiments demonstrated that *ARID1A* deficiency leads to DNA replication stress (Tsai et al., 2020) and impaired checkpoint activation and repair of DNA double-strand breaks (DSBs), which sensitizes to DSB-inducing treatments (Shen et al., 2015). Moreover, ARID1A normally recruits MSH2 to chromatin during DNA replication and promotes mismatch repair (MMR); however, its deficiency is associated with the impairment of MMR and thus an increase in mutagenesis and mutational load (Shen et al., 2018). As a consequence, ARID1A deficiency has been investigated as a biomarker of response to anti-PD-1/PD-L1 immunotherapy treatment (Okamura et al., 2020); alterations in this gene were found to be associated with a longer PFS in patients treated with anti-PD-1/PD-L1 immunotherapy (regardless of microsatellite and tumor mutational burden status). It has been demonstrated that 15% of CUP patients harbor alterations in *ARID1A* gene (MSK impact study; Zehir et al., 2017). Therefore, immune checkpoint inhibitors could be considered as a therapeutic option for ARID1A mutated CUP cases. In the two CUP cases investigated in this study, ARID1A-dependent accumulation of genetic alterations could explain the number of novel mutations that were longitudinally detected in the ccfDNA.

However, another explanation could be that the mutation load was boosted by the mutagenic activity of oxaliplatin (L-OHP), a DNA-alkylating-like agent,

FIGURE 5 | Clustering analysis of 10 CTCs based on whole-genome copy number profile. The heatmap represents the relative copy number profiles of 10 different CTCs isolated through CELLSEARCH® and DEPArray™ technologies. Segments of gains or deletions are color-coded according their relative log2 copy number ratios.
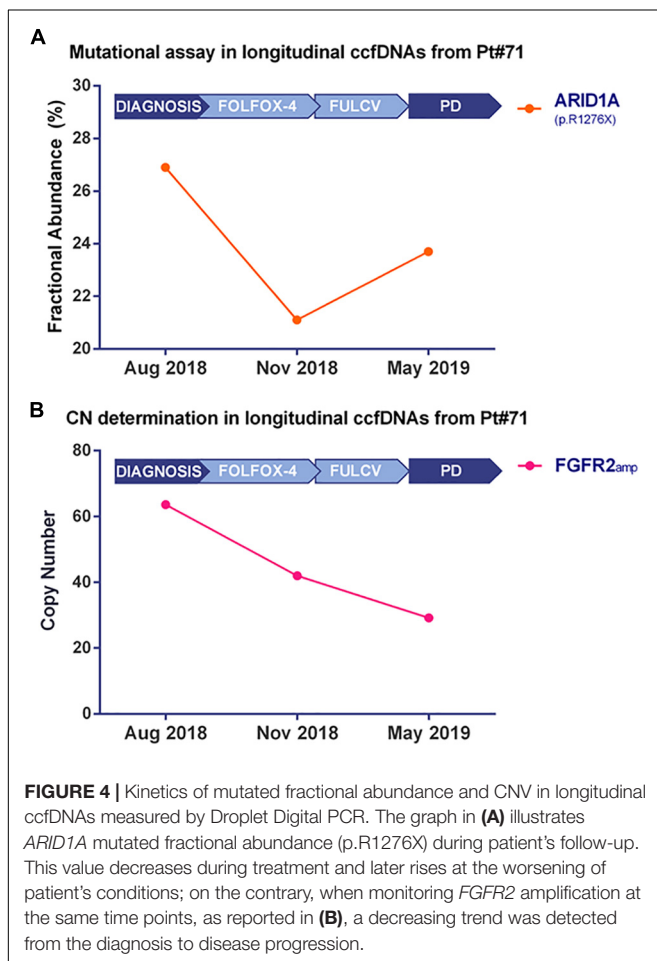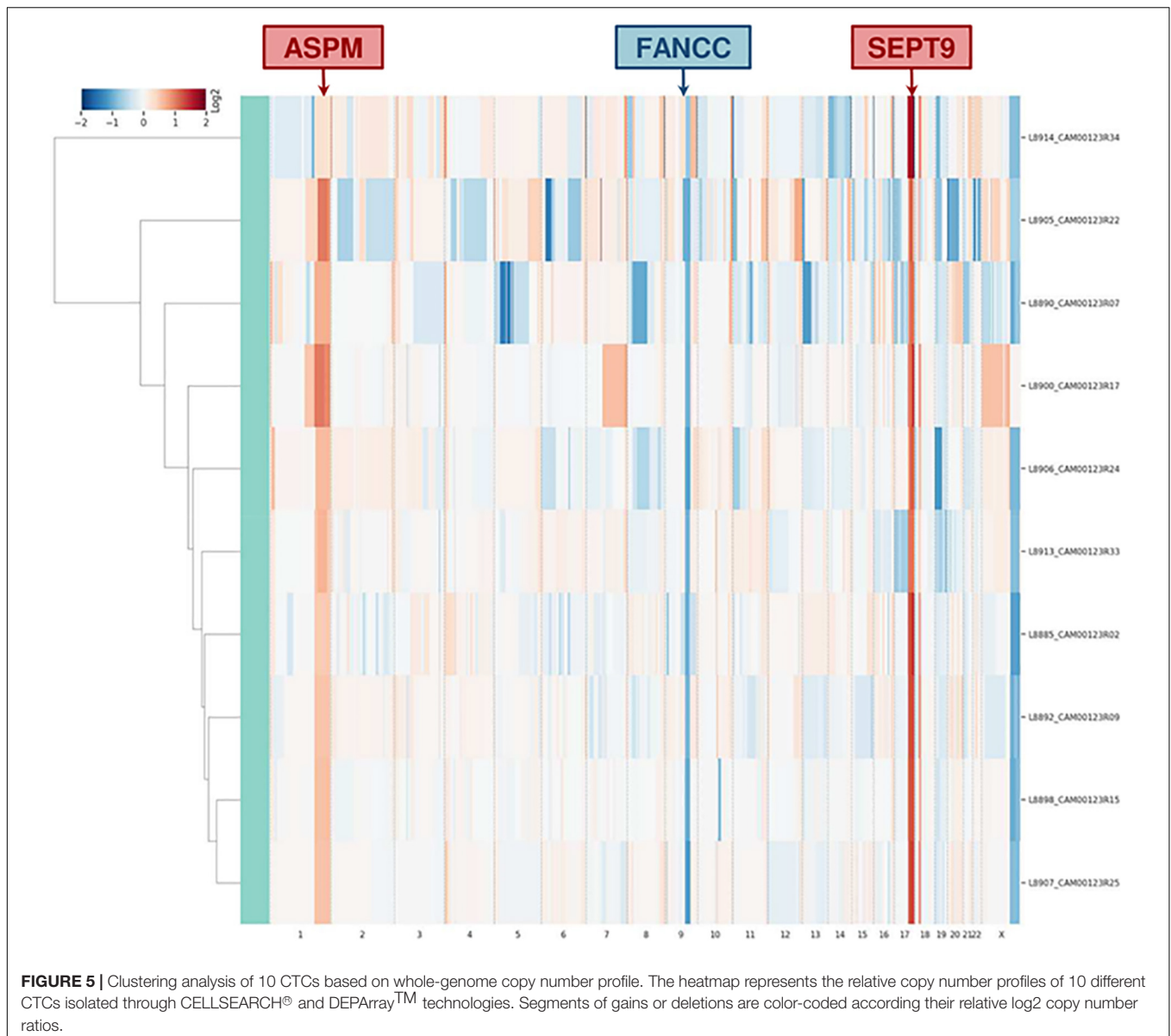
which is included in FOLFOX-4 chemotherapy combination along with Leucovorin and 5-fluorouracil (5-FU) (Silva et al., 2005; Kawamoto et al., 2012). This chemotherapy regimen is commonly used to manage metastatic colorectal cancer (Benson et al., 2014), but also administered to CUP patients with K20$^+$/K7$^-$/CDX2$^+$ IHC signature.

Overall, our analysis constitutes the proof of concept needed to assess the relevance of liquid biopsy genetic testing in metastatic cancer of unknown origin and underlies the importance of using dedicated NGS panels to identify actionable genetic alterations.

Altogether, our results support the use of liquid biopsy, either using CTCs or ccfDNA, in the genetic characterization of CUPs and identification of driver mutations, with the advantage of a minimally invasive approach and potential

longitudinal monitoring. This is a proof-of-concept study on a small number of patients, but given the rarity of the disease and the great need for effective therapies, we believe we provided valuable novel data. We can also conclude that a timely genetic testing and the use of broad or CUP-dedicated NGS panels, covering the most frequently mutated genes, are of the outmost importance to offer these patients novel therapeutic options and potentially improve their survival.

DATA AVAILABILITY STATEMENT

The datasets presented in this article are not readily available because patients have consented to the use of their individual genetic data for biomedical research, but not for unlimited public

data release. Requests to access the datasets should be directed to corresponding author.

ETHICS STATEMENT

The studies involving human participants were reviewed and approved by the Ethics Committee Center Emilia-Romagna Region – Italy (protocol 130/2016/U/Tess). The patients/participants provided their written informed consent to participate in this study.

AUTHOR CONTRIBUTIONS

FUNDING

SUPPLEMENTARY MATERIAL

The Supplementary Material for this article can be found online at: https://www.frontiersin.org/articles/10.3389/fcell.2021.666156/full#supplementary-material

Supplementary Figure 1 | DEPArray NxT representative CTC images from patient #95. Cell gallery acquired by DEPArray, showing single fluorescent channels and overlays, and bright field (BF) images where the DEPArray electrodes (pitch 20µm) are visible.

Supplementary Figure 2 | Patient #71: Low-Pass Whole Genome CNA profiles. **(A)** FFPE without compensation: the signal produced by normal cells impact the copy-number alterations (CNA) call. **(B)** Pure single-CTC: clear CNA calls with digital copy-number values (e.g., Chr 8q $n = 4$). **(C)** FFPE analysis set at 70% normal DNA contamination: signal is amplified and, among increased noise, some true positive CNA detected also in CTCs are called (green arrows) along with putative false-positives (orange arrows).

Supplementary Figure 3 | Mutational assay and copy number determination assay by Droplet Digital PCR. The graph reports ddPCR outputs of *ARID1A* mutated fractional abundance (p.R1276X) **(A)** and in *FGFR2* amplification **(B)** during patient's follow-up at three different time points.

Supplementary Figure 4 | Patient #95 single-CTCs images and CNA profiles. Cell gallery acquired by DEPArray, showing single fluorescent channels and overlays, and bright field (BF) images for 10 CTCs, paired with the corresponding CNA profile.

Supplementary Table 1 | List of genes and regions included in SureSelect custom panel.

REFERENCES

Aceto, N., Bardia, A., Miyamoto, D. T., Donaldson, M. C., Wittner, B. S., Spencer, J. A., et al. (2014). Circulating tumor cell clusters are oligoclonal precursors of breast cancer metastasis. *Cell* 158, 1110–1122. doi: 10.1016/j.cell.2014.07.013

Adzhubei, I. A., Schmidt, S., Peshkin, L., Ramensky, V. E., Gerasimova, A., Bork, P., et al. (2010). A method and server for predicting damaging missense mutations. *Nat Methods* 7, 248–249. doi: 10.1038/nmeth0410-248

Akhter, M. Z., Sharawat, S. K., Kumar, V., Kochat, V., Equbal, Z., Ramakrishnan, M., et al. (2018). Aggressive serous epithelial ovarian cancer is potentially propagated by EpCAM(+)CD45(+) phenotype. *Oncogene* 37, 2089–2103. doi: 10.1038/s41388-017-0106-y

Amintas, S., Bedel, A., Moreau-Gaudry, F., Boutin, J., Buscail, L., Merlio, J. P., et al. (2020). Circulating tumor cell clusters: united we stand divided we fall. *Int. J. Mol. Sci.* 21:2653. doi: 10.3390/ijms21072653

Arai, Y., Totoki, Y., Hosoda, F., Shirota, T., Hama, N., Nakamura, H., et al. (2014). Fibroblast growth factor receptor 2 tyrosine kinase fusions define a unique molecular subtype of cholangiocarcinoma. *Hepatology* 59, 1427–1434. doi: 10.1002/hep.26890

Barber, L. J., Mansukhani, S., Herman, B., Arezi, B., and Gerlinger, M. (2017). *Application Note: Ultra-sensitive Cancer Liquid Biopsy Analysis with the Agilent SureSelectXT HS Target Enrichment Workflow*. Santa Clara, CA: Agilent Technologies.

Benson, A. B. III, Venook, A. P., Bekaii-Saab, T., Chan, E., Chen, Y. J., Cooper, H. S., et al. (2014). Colon cancer, version 3.2014. *J. Natl. Compr. Canc. Netw.* 12, 1028–1059. doi: 10.6004/jnccn.2014.0099

Byron, S. A., Gartside, M., Powell, M. A., Wellens, C. L., Gao, F., Mutch, D. G., et al. (2012). FGFR2 point mutations in 466 endometrioid endometrial tumors: relationship with MSI, KRAS, PIK3CA, CTNNB1 mutations and clinicopathological features. *PLoS One* 7:e30801. doi: 10.1371/journal.pone.0030801

Chakravarty, D., Gao, J., Phillips, S., Kundra, R., Zhang, H., Wang, J., et al. (2017). OncoKB: a precision oncology knowledge base. *JCO Precis. Oncol.* 2017:PO.17.00011. doi: 10.1200/po.17.00011

Chang, J., Liu, X., Wang, S., Zhang, Z., Wu, Z., Zhang, X., et al. (2014). Prognostic value of FGFR gene amplification in patients with different types of cancer: a systematic review and meta-analysis. *PLoS One* 9:e105524. doi: 10.1371/journal.pone.0105524

Chun, S., and Fay, J. C. (2009). Identification of deleterious mutations within three human genomes. *Genome Res* 19, 1553–1561. doi: 10.1101/gr.092619.109

Cinausero, M., Laprovitera, N., De Maglio, G., Gerratana, L., Riefolo, M., Macerelli, M., et al. (2019). KRAS and ERBB-family genetic alterations affect response to PD-1 inhibitors in metastatic nonsquamous NSCLC. *Ther. Adv. Med. Oncol.* 11:1758835919885540. doi: 10.1177/1758835919885540

Cohen, S. J., Punt, C. J., Iannotti, N., Saidman, B. H., Sabbath, K. D., Gabrail, N. Y., et al. (2008). Relationship of circulating tumor cells to tumor response, progression-free survival, and overall survival in patients with metastatic colorectal cancer. *J. Clin. Oncol.* 26, 3213–3221. doi: 10.1200/JCO.2007.15.8923

Conway, A. M., Mitchell, C., and Cook, N. (2019). Challenge of the unknown: how can we improve clinical outcomes in cancer of unknown primary? *J. Clin. Oncol.* 37, 2089–2090. doi: 10.1200/jco.19.00449

Cristofanilli, M., Budd, G. T., Ellis, M. J., Stopeck, A., Matera, J., Miller, M. C., et al. (2004). Circulating tumor cells, disease progression, and survival in metastatic breast cancer. *N. Engl. J. Med.* 351, 781–791. doi: 10.1056/NEJMoa040766

Deng, N., Goh, L. K., Wang, H., Das, K., Tao, J., Tan, I. B., et al. (2012). A comprehensive survey of genomic alterations in gastric cancer reveals

systematic patterns of molecular exclusivity and co-occurrence among distinct therapeutic targets. *Gut* 61, 673–684. doi: 10.1136/gutjnl-2011-301839

Dienstmann, R., Rodon, J., Prat, A., Perez-Garcia, J., Adamo, B., Felip, E., et al. (2014). Genomic aberrations in the FGFR pathway: opportunities for targeted therapies in solid tumors. *Ann. Oncol.* 25, 552–563. doi: 10.1093/annonc/mdt419

Douville, C., Masica, D. L., Stenson, P. D., Cooper, D. N., Gygax, D. M., Kim, R., et al. (2016). Assessing the pathogenicity of insertion and deletion variants with the variant effect scoring tool (VEST-Indel). *Hum. Mutat.* 37, 28–35. doi: 10.1002/humu.22911

Drapkin, B. J., George, J., Christensen, C. L., Mino-Kenudson, M., Dries, R., Sundaresan, T., et al. (2018). Genomic and functional fidelity of small cell lung cancer patient-derived xenografts. *Cancer Discov.* 8, 600–615. doi: 10.1158/2159-8290.CD-17-0935

Fizazi, K., Greco, F. A., Pavlidis, N., Daugaard, G., Oien, K., Pentheroudakis, G., et al. (2015). Cancers of unknown primary site: ESMO clinical practice guidelines for diagnosis, treatment and follow-up. *Ann. Oncol.* 26(Suppl. 5), v133–v138. doi: 10.1093/annonc/mdv305

Haratani, K., Hayashi, H., Takahama, T., Nakamura, Y., Tomida, S., Yoshida, T., et al. (2019). Clinical and immune profiling for cancer of unknown primary site. *J. Immunother. Cancer* 7:251. doi: 10.1186/s40425-019-0720-z

Huang, X., Wu, H. M., Zhu, C., Shao, D., Guo, D., Zhou, Y., et al. (2020). Next generation sequencing reveals CCNE1 amplification as an independent prognostic factor for triple negative breast cancer (TNBC) patients. *J. Clin. Oncol.* 38:558. doi: 10.1200/JCO.2020.38.15_suppl.558

Ignatiadis, M., and Dawson, S. J. (2014). Circulating tumor cells and circulating tumor DNA for precision medicine: dream or reality? *Ann. Oncol.* 25, 2304–2313. doi: 10.1093/annonc/mdu480

Joosse, S. A., Gorges, T. M., and Pantel, K. (2015). Biology, detection, and clinical implications of circulating tumor cells. *EMBO Mol. Med.* 7, 1–11. doi: 10.15252/emmm.201303698

Kadoch, C., Hargreaves, D. C., Hodges, C., Elias, L., Ho, L., Ranish, J., et al. (2013). Proteomic and bioinformatic analysis of mammalian SWI/SNF complexes identifies extensive roles in human malignancy. *Nat. Genet.* 45, 592–601. doi: 10.1038/ng.2628

Karczewski, K. J., Francioli, L. C., Tiao, G., Cummings, B. B., Alfoldi, J., Wang, Q., et al. (2020). The mutational constraint spectrum quantified from variation in 141,456 humans. *Nature* 581, 434–443. doi: 10.1038/s41586-020-2308-7

Kato, S., Krishnamurthy, N., Banks, K. C., De, P., Williams, K., Williams, C., et al. (2017). Utility of genomic analysis in circulating tumor DNA from patients with carcinoma of unknown primary. *Cancer Res.* 77, 4238–4246. doi: 10.1158/0008-5472.CAN-17-0628

Kawamoto, Y., Tsuchihara, K., Yoshino, T., Ogasawara, N., Kojima, M., Takahashi, M., et al. (2012). KRAS mutations in primary tumours and post-FOLFOX metastatic lesions in cases of colorectal cancer. *Br. J. Cancer* 107, 340–344. doi: 10.1038/bjc.2012.218

Kircher, M., Witten, D. M., Jain, P., O'Roak, B. J., Cooper, G. M., and Shendure, J. (2014). A general framework for estimating the relative pathogenicity of human genetic variants. *Nat. Genet.* 46, 310–315. doi: 10.1038/ng.2892

Komine, K., Inoue, M., Otsuka, K., Fukuda, K., Nanjo, H., and Shibata, H. (2014). Utility of measuring circulating tumor cell counts to assess the efficacy of treatment for carcinomas of unknown primary origin. *Anticancer Res.* 34, 3165–3168.

Laprovitera, N., Riefolo, M., Ambrosini, E., Klec, C., Pichler, M., and Ferracin, M. (2021). Cancer of unknown primary: challenges and progress in clinical management. *Cancers* 13:451. doi: 10.3390/cancers13030451

Lucci, A., Hall, C. S., Lodhi, A. K., Bhattacharyya, A., Anderson, A. E., Xiao, L., et al. (2012). Circulating tumour cells in non-metastatic breast cancer: a prospective study. *Lancet Oncol.* 13, 688–695. doi: 10.1016/S1470-2045(12)70209-7

Matsusaka, S., Chin, K., Ogura, M., Suenaga, M., Shinozaki, E., Mishima, Y., et al. (2010). Circulating tumor cells as a surrogate marker for determining response to chemotherapy in patients with advanced gastric cancer. *Cancer Sci.* 101, 1067–1071. doi: 10.1111/j.1349-7006.2010.01492.x

Nakayama, N., Nakayama, K., Shamima, Y., Ishikawa, M., Katagiri, A., Iida, K., et al. (2010). Gene amplification CCNE1 is related to poor survival and potential

therapeutic target in ovarian cancer. *Cancer* 116, 2621–2634. doi: 10.1002/cncr.24987

Okamura, R., Kato, S., Lee, S., Jimenez, R. E., Sicklick, J. K., and Kurzrock, R. (2020). ARID1A alterations function as a biomarker for longer progression-free survival after anti-PD-1/PD-L1 immunotherapy. *J. Immunother. Cancer.* 8:e000438. doi: 10.1136/jitc-2019-000438

Pairawan, S., Hess, K. R., Janku, F., Sanchez, N. S., Mills Shaw, K. R., Eng, C., et al. (2020). Cell-free circulating tumor DNA variant allele frequency associates with survival in metastatic cancer. *Clin. Cancer Res.* 26, 1924–1931. doi: 10.1158/1078-0432.CCR-19-0306

Povysil, G., Tzika, A., Vogt, J., Haunschmid, V., Messiaen, L., Zschocke, J., et al. (2017). panelcn.MOPS: copy-number detection in targeted ngs panel data for clinical diagnostics. *Hum. Mutat.* 38, 889–897. doi: 10.1002/humu.23237

Reva, B., Antipin, Y., and Sander, C. (2011). Predicting the functional impact of protein mutations: application to cancer genomics. *Nucleic Acids Res.* 39:e118. doi: 10.1093/nar/gkr407

Riethdorf, S., Fritsche, H., Muller, V., Rau, T., Schindlbeck, C., Rack, B., et al. (2007). Detection of circulating tumor cells in peripheral blood of patients with metastatic breast cancer: a validation study of the cell search system. *Clin. Cancer Res.* 13, 920–928. doi: 10.1158/1078-0432.CCR-06-1695

Ross, J. S., Wang, K., Gay, L., Otto, G. A., White, E., Iwanik, K., et al. (2015). Comprehensive genomic profiling of carcinoma of unknown primary site: new routes to targeted therapies. *JAMA Oncol.* 1, 40–49. doi: 10.1001/jamaoncol.2014.216

Schwarz, J. M., Cooper, D. N., Schuelke, M., and Seelow, D. (2014). MutationTaster2: mutation prediction for the deep-sequencing age. *Nat. Methods* 11, 361–362. doi: 10.1038/nmeth.2890

Seo, S., Park, S. J., Ryu, M. H., Park, S. R., Ryoo, B. Y., Park, Y. S., et al. (2017). Prognostic impact of fibroblast growth factor receptor 2 gene amplification in patients receiving fluoropyrimidine and platinum chemotherapy for metastatic and locally advanced unresectable gastric cancers. *Oncotarget* 8, 33844–33854. doi: 10.18632/oncotarget.12953

Shen, J., Ju, Z., Zhao, W., Wang, L., Peng, Y., Ge, Z., et al. (2018). ARID1A deficiency promotes mutability and potentiates therapeutic antitumor immunity unleashed by immune checkpoint blockade. *Nat. Med.* 24, 556–562. doi: 10.1038/s41591-018-0012-z

Shen, J., Peng, Y., Wei, L., Zhang, W., Yang, L., Lan, L., et al. (2015). ARID1A deficiency impairs the dna damage checkpoint and sensitizes cells to parp inhibitors. *Cancer Discov.* 5, 752–767. doi: 10.1158/2159-8290.cd-14-0849

Shihab, H. A., Gough, J., Cooper, D. N., Stenson, P. D., Barker, G. L., Edwards, K. J. I, et al. (2013). Predicting the functional, molecular, and phenotypic consequences of amino acid substitutions using hidden Markov models. *Hum. Mutat.* 34, 57–65. doi: 10.1002/humu.22225

Silva, M. J., Costa, P., Dias, A., Valente, M., Louro, H., and Boavida, M. G. (2005). Comparative analysis of the mutagenic activity of oxaliplatin and cisplatin in the Hprt gene of CHO cells. *Environ. Mol. Mutagen.* 46, 104–115. doi: 10.1002/em.20138

Silverman, I. M., Murugesan, K., Lihou, C. F., Féliz, L., Frampton, G. M., Newton, R. C., et al. (2019). Comprehensive genomic profiling in FIGHT-202 reveals the landscape of actionable alterations in advanced cholangiocarcinoma. *J. Clin. Oncol.* 37(15 Suppl.):4080. doi: 10.1200/JCO.2019.37.15_suppl.4080

Sparano, J., O'Neill, A., Alpaugh, K., Wolff, A. C., Northfelt, D. W., Dang, C. T., et al. (2018). Association of circulating tumor cells with late recurrence of estrogen receptor-positive breast cancer: a secondary analysis of a randomized clinical trial. *JAMA Oncol.* 4, 1700–1706. doi: 10.1001/jamaoncol.2018.2574

Tanizaki, J. Y., Akiyoshi, K., Minami, K., Ueda, H., Takiguchi, H., Nakayama Kondoh, H., et al. (2020). NivoCUP: an open-label phase II study on the efficacy of nivolumab in cancer of unknown primary. *J. Clin. Oncol.* 38(15 Suppl.):106. doi: 10.1200/JCO.2020.38.15_suppl.106

Trizzino, M., Barbieri, E., Petracovici, A., Wu, S., Welsh, S. A., Owens, T. A., et al. (2018). The tumor suppressor arid1a controls global transcription via pausing of RNA Polymerase II. *Cell Rep.* 23, 3933–3945. doi: 10.1016/j.celrep.2018.05.097

Tsai, S., Chang, E. Y.-c., Fournier, L.-A., Wells, J. P., Minaker, S. W., Zhu, Y. D., et al. (2020). ARID1A regulates R-loop associated DNA replication stress. *bioRxiv* [Preprint]. doi: 10.1101/2020.11.16.384446

Turner, N., and Grose, R. (2010). Fibroblast growth factor signalling: from development to cancer. *Nat. Rev. Cancer* 10, 116–129. doi: 10.1038/nrc2780

Varadhachary, G. R., and Raber, M. N. (2014). Cancer of unknown primary site. *N. Engl. J. Med.* 371, 757–765. doi: 10.1056/NEJMra1303917

Varghese, A. M., Arora, A., Capanu, M., Camacho, N., Won, H. H., Zehir, A., et al. (2017). Clinical and molecular characterization of patients with cancer of unknown primary in the modern era. *Ann. Oncol.* 28, 3015–3021. doi: 10.1093/annonc/mdx545

Vaser, R., Adusumalli, S., Leng, S. N., Sikic, M., and Ng, P. C. (2016). SIFT missense predictions for genomes. *Nat. Protoc.* 11, 1–9. doi: 10.1038/nprot.2015.123

Wang, K., Li, M., and Hakonarson, H. (2010). ANNOVAR: functional annotation of genetic variants from high-throughput sequencing data. *Nucleic Acids Res.* 38:e164. doi: 10.1093/nar/gkq603

Yu, M., Bardia, A., Aceto, N., Bersani, F., Madden, M. W., Donaldson, M. C., et al. (2014). Cancer therapy. ex vivo culture of circulating breast tumor cells for individualized testing of drug susceptibility. *Science* 345, 216–220. doi: 10.1126/science.1253533

Yu, M., Stott, S., Toner, M., Maheswaran, S., and Haber, D. A. (2011). Circulating tumor cells: approaches to isolation and characterization. *J. Cell Biol.* 192, 373–382. doi: 10.1083/jcb.201010021

Zehir, A., Benayed, R., Shah, R. H., Syed, A., Middha, S., Kim, H. R., et al. (2017). Mutational landscape of metastatic cancer revealed from prospective clinical sequencing of 10,000 patients. *Nat. Med.* 23, 703–713. doi: 10.1038/nm.4333

Zhao, P., Zhou, W., Liu, C., Zhang, H., Cheng, Z., Wu, W., et al. (2019). Establishment and characterization of a CTC cell line from peripheral blood of breast cancer patient. *J. Cancer* 10, 6095–6104. doi: 10.7150/jca.33157